Astron. Astrophys. 60, 327—336 (1977)

ASTRONOMY AND ASTROPHYSICS

Propagation of Magnetohydrodynamic Waves from the Galactic Center

Origin of the 3-kpc Arm and the North Polar Spur

Yoshiaki Sofue*

Max-Planck-Institut für Radioastronomie, Auf dem Hügel 69, D-5300 Bonn, Federal Republic of Germany

Received March 2, 1977

Summary. Magnetohydrodynamic waves isotropically radiated from the galactic center are reflected in the galactic halo, and more than 80% of the wave front focuses on a ring in the galactic disk. Due to the focusing effect, a compression wave of small amplitude developes into a strong shock as it approaches the ring, which may explain the 3-kpc arm. The radius of the ring is 3.5 kpc if a scale-height of variation of the Alfvén velocity is specified as 1.7 kpc.

A small portion of the wave front escapes into the galactic corona, where the front forms a large shell structure. A tangential view of this shell from the sun could be responsible for the North Polar Spur. This picture agrees with the fact that the smooth extension of the NPS-ridge crosses the galactic plane at $l=21°$, which coincides with the tangential direction of the 3-kpc arm.

Key words: galactic activity — galactic corona — MHD waves — North Polar Spur — 3-kpc arm

I. Introduction

The 3 kpc expanding arm at a galactocentric distance of $\varpi=3.5$ kpc found in the 21-cm line emission (Rougoor, 1964) has been investigated theoretically in two ways: first in relation to an explosive phenomenon at the galactic nucleus (van der Kruit, 1971; Lynden-Bell and Rees, 1971; Sanders and Prendergast, 1974; Sofue, 1976a: this paper is referred to as Paper I; Saito, 1976); and second in relation to a dispersion ring at the inner Lindblad resonance of the density waves (Simonson and Mader, 1973). In the present paper, we discuss the origin of the 3-kpc arm on the basis of the explosion hypothesis with special reference to propagation of MHD (magnetohydrodynamic) shock waves from the galactic center through the galactic disk and halo. The MHD model proposed in Paper I is improved by adopting a more realistic structure of the galactic corona.

We also examine the influence of the MHD shock waves on the background radio emission and discuss the origin of the North Polar Spur (NPS). The NPS seems to be distinguished from other galactic spurs by its high radio brightness along the narrow ridge [see e.g., maps at 820 MHz by Berkhuijsen (1972); and at 408 MHz by Haslam et al. (1974)]. The other spurs, including Loops II, III and many smaller spurs emerging from the galactic plane, can be naturally reproduced in our model based on the galactic shock hypothesis (Sofue, 1973; Sofue et al., 1974, 1976; Sofue, 1976b). In the course of our spur studies, we have pointed out that the smooth extension of the NPS ridge crosses the galactic plane at $l=21°$ which coincides with the tangential direction of the 3-kpc arm. In the present paper, we try to account for the NPS in terms of a magnetohydrodynamical phenomenon of galactic scale associated with the galactic center activity.

II. Focussing MHD Wave Hypothesis for the 3-kpc Arm

In Paper I, we have proposed a mechanism that causes a ring structure in the gaseous disk of the Galaxy: Magnetohydrodynamical disturbances originating at the galactic center propagate through the galactic halo and the disk. They converge into a ring in the disk apart from the center. The convergence occurs at a high efficiency of more than 90%. The convergence (or focal) ring appears at 3.5 kpc of the galactic center, if the scale thickness H of the distribution of the Alfvén velocity V, defined through $V=V_0\exp(z/H)^2$, is taken to be 1.7 kpc. Here V_0 is the Alfvén velocity at the galactic plane and z is the distance from the plane. In this and the following sections, we improve the MHD model on the basis of more realistic distribution of Alfvén velocity in the higher galactic corona.

(i) MHD *Waves in the Galaxy*

A method to trace the propagation of MHD waves in a magnetized plasma has been developed by Uchida (1970,

* Senior von Humboldt Fellow on absence of Department of Physics, Nagoya University, Nagoya, Japan

1975) and Uchida et al. (1973). The method was primarily introduced to study the coronal magnetic structure of the sun by making use of the Moreton's wave (Moreton, 1960; Uchida, 1968). In this paper, instead, we apply the method to the galactic center region, as has already been attempted in Paper I.

For simplicity we assume an axisymmetry around the galactic rotation axis (z-axis). Nondimensional equations describing the propagation of a fast-mode MHD wave packet are written as follows (Uchida, 1970; Paper I):

$$\frac{d\xi}{d\tau}=\frac{Fp_r}{p}, \tag{1}$$

$$\frac{d\theta}{d\tau}=\frac{Fp_\theta}{p\xi}, \tag{2}$$

$$\frac{dp_r}{d\tau}=-p\frac{\partial F}{\partial \xi}+F\frac{p_\theta^2}{p\xi}, \tag{3}$$

$$\frac{dp_\theta}{d\tau}=-\frac{p}{\xi}\frac{\partial F}{\partial \theta}-F\frac{p_\theta p_r}{p\xi}, \tag{4}$$

$$\xi=r/H, \quad \tau=t/(H/V_0), \tag{5}$$

$$F=\frac{V(r,\theta)}{V_0}, \tag{6}$$

and

$$p=\sqrt{p_r^2+p_\theta^2}. \tag{7}$$

Here (r,θ) are the polar coordinates of the position of the wave packet, H the scale factor with a dimension of length, and t is the time. The vector $\boldsymbol{p}=(p_r,p_\theta)$ is defined through $\boldsymbol{p}=\mathrm{grad}\,\Phi$, where Φ is the eikonal or the phase function of the wave. The Alfvén velocity $V(r,\theta)$ is a model-dependent function of r and θ.

The above equations are valid for the fast-mode waves insofar as the requirement, $V^2\gg a^2$, is satisfied, where a is the sound velocity (Uchida, 1970). This requirement is met in the galactic center region (Paper I). The propagation of the fast-mode wave is then independent of the magnetic field orientation, and depends only on the distribution of the Alfvén velocity V. In this case, dissipation of the wave has been shown to be negligible provided that the wave amplitude is small (Paper I).

(ii) Distribution of the Alfvén Velocity

As we did in Paper I, we assume again that the distribution of the Alfvén velocity is stratified and parallel to the galactic plane, or V is a function of z alone. In Paper I, we assumed that the velocity has the form of $V=V_0\exp(z/H)^2$ with $H=1.7$ kpc. This value of H is reasonable as can be seen from the following consideration: Although most of the galactic magnetic field is frozen in the interstellar gas, it seems reasonable to assume that the scale-thickness h_m of the magnetic field may be slightly larger than that h_g of the gaseous disk, because the magnetic field tends to inflate out of the disk due to Parker type instabilities (Parker, 1969). If the magnetic pressure and electron density vary with z as $\exp(-z^2/h_m^2)$ and $\exp(-z^2/h_g^2)$, respectively, then the Alfvén velocity varies with z as $V\propto\exp(z^2/H^2)$ with $H=\sqrt{2h_mh_g/(h_m^2-h_g^2)^{1/2}}$. If we take that h_m is greater than h_g only by 0.3 %, we have $H=1.7$ kpc. Here we assumed that $h_g=100$ pc.

We assume the following two cases as model distributions of the Alfvén velocity:

$$\text{Case A:}\quad V(z)=V_0\exp(z/H)^2 \tag{8}$$

$$\text{Case B:}\quad V(z)=V_0\exp[(z/H)^2/(1+\alpha(z/H)^2)] \tag{9}$$

where α is a constant.

Case A is the same as discussed in Paper I. In Case B, the Alfvén velocity increases monotonically with z, but tends to a slowly varying function of z, finally reaching a constant value, $V_0\exp(1/\alpha)$, at high z. Although there has never been an accurate model of the magnetohydrodynamical structure of our galactic halo or corona (Woltjer, 1965), Case B seems more plausible than A, because it is unlikely that the Alfvén velocity increases so steeply to infinity with z as in Case A.

III. Propagation of the MHD Wave Front through the Galactic Disk and Corona

We present the results of numerical computations of the wave propagations in Cases A and B. We here take that $H=1.7$ kpc and $V_0=20\,\mathrm{km\,s^{-1}}$ following Paper I.

(i) Case A

This simple case has already been discussed in Paper I in detail. The MHD disturbances originating at the nucleus of the Galaxy propagate through the galactic halo and all of the waves are reflected at high-z regions. Most of the waves focus on a ring in the gaseous disk at $\varpi=3.5$ kpc. The energy liberated at the galactic center converges into the ring with an efficiency of 98 %. Such a high efficiency has been shown to be a promising mechanism to give rise to the 3-kpc arm (Paper I). We show the result in Figure 1, in which wave fronts are portrayed as seen from a galactocentric latitude of 30°.

(ii) Case B

If the Galaxy has an extended corona with gas and magnetic fields, the Alfvén velocity would not increase infinitely with z, but tend to a finite value. We here assume such a magnetic corona, and take the form expressed by Equation (9) for the Alfvén velocity, where V tends to a finite value, $V_\infty=V_0\exp(1/\alpha)$, in regions at high z.

We compute the propagations of MHD waves for the following parameter values: $\alpha=0.4$ ($V_\infty=244\,\mathrm{km\,s^{-1}}$); $\alpha=0.5$ ($V_\infty=150\,\mathrm{km\,s^{-1}}$); $\alpha=0.6$ ($V_\infty=100\,\mathrm{km\,s^{-1}}$) and $\alpha=0.7$ ($V_\infty=80\,\mathrm{km\,s^{-1}}$). Figure 2a shows the time development of the wave front for $\alpha=0.5$. Figure 2b shows

the same result projected in galactic coordinates as seen from the sun. Figure 3 compares the wave fronts for (a) $\alpha=0$, (b) 0.4, (c) 0.5 and (d) 0.7 at $t=5$, 10 and 18.10^7 years.

Approximately 80% of the MHD wave front focuses on the narrow ring near $\varpi=3.5$ kpc at $t=17-20.10^7$ years as in Case A. However the remaining 30% of the front expands almost spherically into the corona at $t\gtrsim 10.10^7$ years and forms a large shell structure in the corona. This shell structure is discussed in Section V in relation to radio background features, in particular to the North Polar Spur. As shown later, the parameter α is likely to be around 0.5 ($V_\infty=150$ km s^{-1}).

IV. Propagation of Blast Shock Waves near the Galactic Plane

We have so far discussed the propagation of MHD waves from the galactic center. The waves converge into a focal ring located at $\varpi\approx 2H$ from the center. In Paper I, we have given an order-of-magnitude estimate of the wave energy required for a galactic center explosion to drive the 3-kpc expanding motion.

To explain the formation of the 3-kpc arm, some authors have attempted to trace shock waves associated with an explosion of the galactic nucleus, by making use of the hydrodynamic methods (Sanders and Prendergast, 1974; Saito, 1976). In what follows, we examine the behaviour of a shock wave propagating near the galactic plane, regarding the galactic disk as a wave duct as shown below. We here approximate the fast-mode MHD wave by a compression wave in isothermal gas including the magnetic pressure.

(i) Galactic Disk as a Wave Duct

As shown in the preceeding sections, wave packets propagating near the galactic plane, or "near-axis rays", coverge into the focal ring. If $z\ll H$, we can analytically integrate Equations (1)–(7) for the Alfvén velocity distribution as given by Equation (8) or (9): we obtain the following ray path:

$$z=C\sin(\sqrt{2}\varpi/H), \tag{10}$$

where C is a constant of integration, and is related to the projection angle θ_0 of the ray with the galactic plane at the nucleus through $C=(H/\sqrt{2})\tan\theta_0$. The focal ring appears at $\varpi_0=(\pi/\sqrt{2})H$, independent of the ray path.

Equation (10), therefore, can be regarded as a form of a "duct" of the MHD waves radiated at small angles to the galactic plane. We then examine a development of density and velocity amplitudes of a blast wave produced at the galactic center and propagating through this wave duct. The cross section of the duct, or the surface area of the wave front, is given by

$$S=2\pi\varpi C\sin(\sqrt{2}\pi\varpi/H). \tag{11}$$

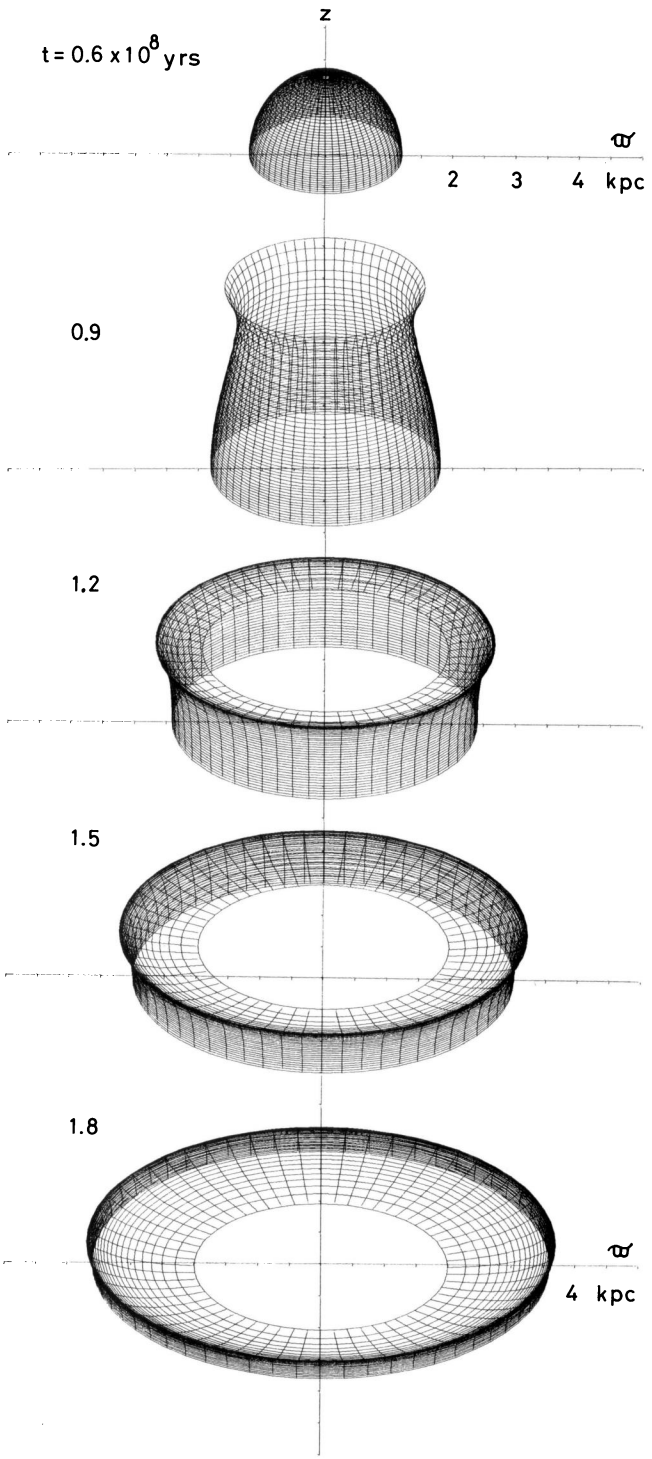

Fig. 1. Bird's eye view of the MHD wave front in Case A as seen from a galactocentric latitude of 30°. Most of the wave front focuses on a ring in the disk at $t=1.8-2.0\,10^8$ years

(ii) Basic Equations for Numerical Integrations

We follow the motion of the compression blast wave in the isothermal gas including magnetic pressure by solving hydrodynamic equations in a Lagrangean scheme. If we denote the Lagrangean and corresponding Eulerian

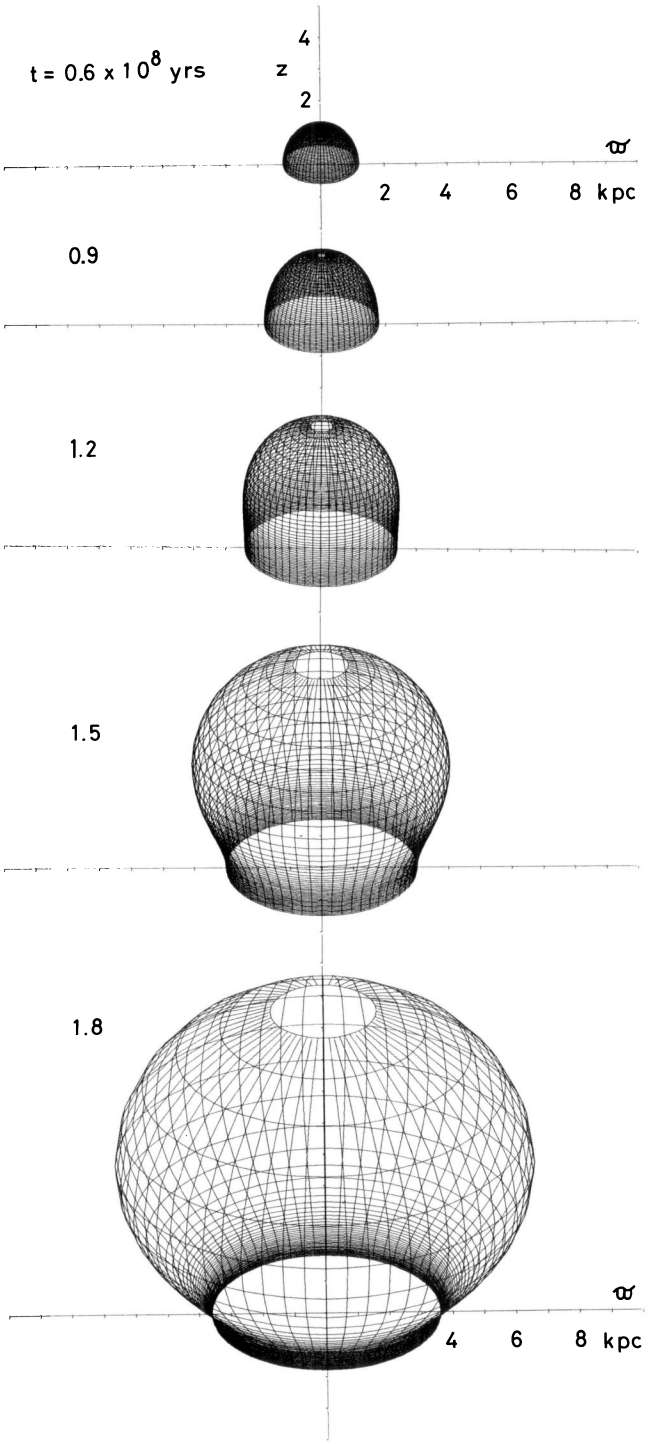

Fig. 2a. The same as Figure 1 but for Case B. A small portion (~20%) of the wave front expands spherically into the galactic corona, while most of the front (~80%) converges into a ring in the disk just as in Case A

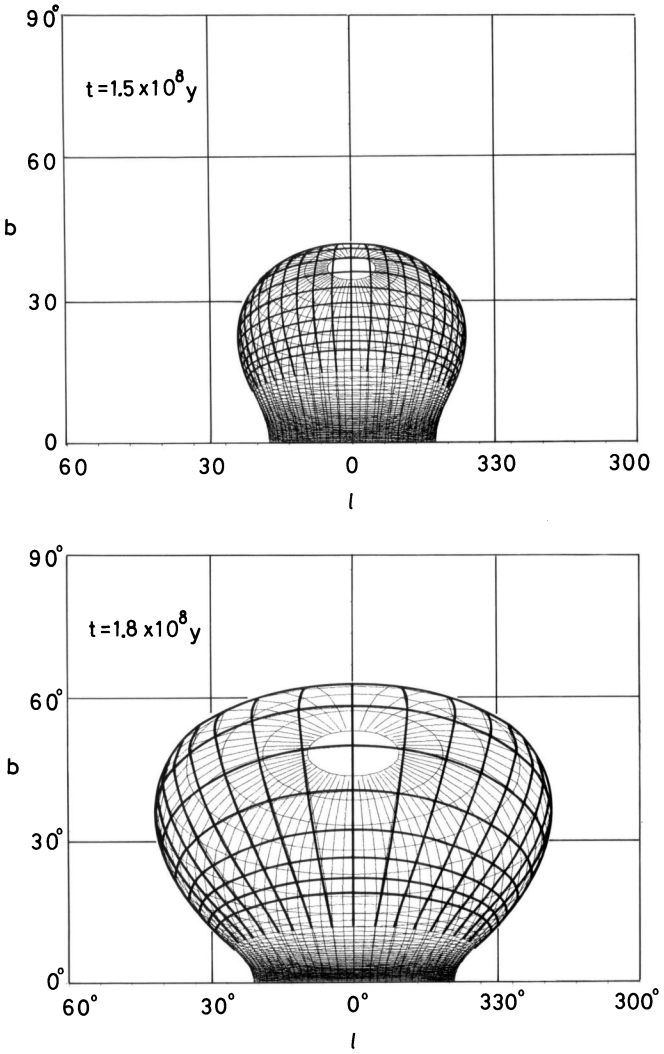

Fig. 2b. The same as Figure 2a but as seen from the sun projected onto the sky in the galactic coordinates system

coordinates of a fluid cell by X and x, respectively, with its velocity u, the equations are written as follows (Richtmeyer, 1957):

$$\frac{\partial X}{\partial t} = u \tag{12}$$

and

$$\frac{\partial u}{\partial t} = -\left(\frac{S}{s}\right)\frac{\partial (P+Q)}{\partial x} w + \frac{h^2(x)}{X^3} - K(X). \tag{13}$$

Here P and Q are the pressure and an artificial viscosity; $h(X) = h(x)$ is the angular momentum which is conserved through the computation; and $K(X)$ is the centrifugal force due to the galactic gravitational field. When $X = x$, the last two terms in Equation (13) are balancing with each other, or $h(x)/x^3 = K(x)$. Surface areas at X and x of the fluid cell are denoted by S and s. The factor S/s in (13) is equal to X^2/x^2 when the calculation is in a spherical symmetric case, equal to X/x when cylindrical, and unity when plane parallel. In our case, however, the surface area varies as Equation (11) and the factor S/s has been modified so that

$$\frac{S}{s} = \frac{X}{x}\frac{\sin(\pi X/\varpi_0)}{\sin(\pi x/\varpi_0)}. \tag{14}$$

We assumed here that the basic structure of the duct remains unchanged in the moving Lagrangean coordinates. Near the galactic center, we have X and $x \ll \varpi_0$, which yields $S/s \approx (X/x)^2$ corresponding to a spherical explosion; for $X \sim \varpi_0/2$, we have $S/s \approx X/x$ corresponding to a cylindrical expansion; and near the focal ring, we have $S/s \approx X'/x'$ with $X' = \varpi_0 - X \ll \varpi_0$ and $x' = \varpi_0 - x \ll \varpi_0$, which corresponds again to a cylindrical approximation around the ring. Here ϖ_0 denotes the distance of the ring from the center.

The variation of a specific volume is then given by

$$W = w\left(\frac{S}{s}\right)\frac{\partial X}{\partial x}, \tag{15}$$

and is related to the gas pressure P_g and temperature T through

$$P_g = T/W. \tag{16}$$

As we have assumed an isothermal case, T is constant everywhere. Finally, the pressure P in Equation (13) is given through

$$P = P_g + P_m \quad \text{with} \quad P_m = P_{m0}\left(\frac{W}{w}\right)^{-4/3}, \tag{17}$$

where P_m is the magnetic pressure and P_{m0} its unperturbed value. The last relation comes from an assumption that the magnetic fields are frozen in the gas, and the magnetic flux conserves. The adiabatic exponent of $-4/3$ is valid for tangled fields, and this applies also to a longitudinal field orientation if the compression is radial.

We now integrate these equations as an initial value problem using the difference method (Richtmeyer, 1957).

At the initial stage, the gas density is taken a constant throughout the wave duct, and the gas is in a static state balancing its centrifugal force with the gravitation. Then a central portion of the gas is given a large expanding motion with supersonic velocity in order to simulate an explosion at the galactic center.

(iii) Propagation of Shock Waves

Figure 4 shows an example of the results of numerical computations, where the initial explosion velocity was taken as five times the sound velocity. The magnetic pressure of the unperturbed state is taken the same as the gas pressure.

As soon as the integration starts, a strong shock wave grows. Then the wave amplitude decreases as it propagates, mainly due to the increase of the cross section of the duct, namely, due to a spherical damping. The wave eventually tends to a blast wave of small amplitude, which propagates without significant dissipation until it approaches the focus. As the wave approaches the focus, or $\varpi \cong \varpi_0$, the amplitude increases rapidly due to the steep decrease of the front surface. Finally, the wave developes again into a strong shock with a high compression. A maximum density of three

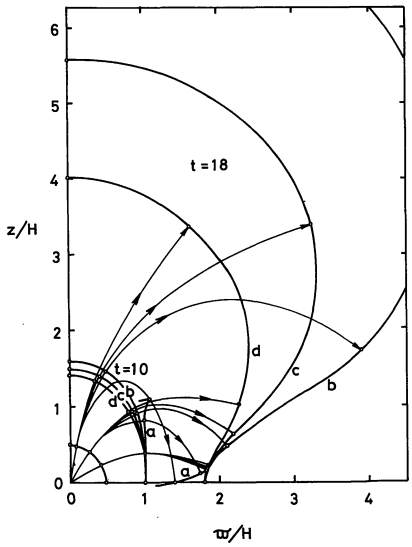

Fig. 3. Propagation of MHD wave fronts on the $(\varpi - z)$ plane for Case A (a) $\alpha = 0$, and for Case B (b) $\alpha = 0.4$ ($V_\infty = 244\,\mathrm{km\,s^{-1}}$); (c) $\alpha = 0.5$ ($V_\infty = 150\,\mathrm{km\,s^{-1}}$); and (d) $\alpha = 0.7$ ($V_\infty = 80\,\mathrm{km\,s^{-1}}$)

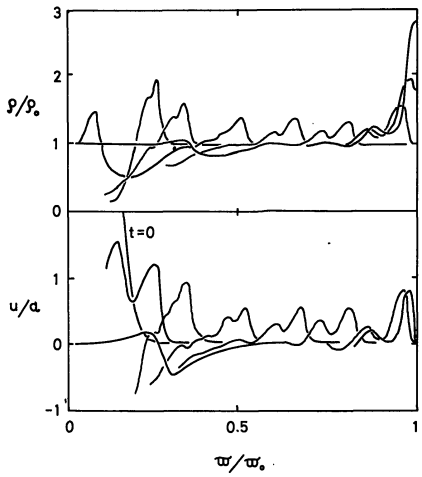

Fig. 4. Propagation of a blast wave from the galactic center region through the disk guided by a wave duct given by Equation (10). Density and velocity amplitudes are shown. Note that the wave grows into a strong shock as it approaches the focal ring at $\varpi = \varpi_0$

times the unperturbed density is obtained. Note that the growth of the shock near the focus is similar to a cylindrical implosion. The shock at the focal ring may be the cause of the 3-kpc expanding arm.

The velocity amplitude u also increases as the front approaches the focus. However, the amplitude reaches at most the amplitude of the local sound velocity, smaller than the observed expansion velocity. This comes from the restriction that the ring is fixed to space, or $u = 0$ at $\varpi = \varpi_0$. Higher velocity amplitudes could be obtained if this condition is removed at the focus.

We also computed the shock propagation for some other parameter combinations. The situation of the wave propagation and variation of the amplitudes was essen-

tially the same even for higher explosion velocities at the nucleus. Even in such violent cases, the density at the focal ring increases at most by four to five times the unperturbed density. It is also remarkable that the gaseous disk behind the shock remains quiet.

Figure 5 shows the variation of an excess of the front density over the unperturbed density as a function of the galactocentric distance. Also plotted is the inverse of the surface area of the wave front, namely, $1/S$, where S is given by Equation (11). The wave amplitude is inversely proportional to S. The energy released by the galactic center explosion is transmitted mostly in a form of a small-amplitude wave: The wave does not suffer from a significant dissipation, and does not strongly disturb the intervening gaseous disk until it reaches the 3-kpc arm.

The present model can save the energy of the galactic center explosion required to explain the velocity of the 3-kpc arm: Since most ($>80\%$) of the energy released in the galactic nucleus converges into the focal ring, the total energy for the explosion at the nucleus would be of the order of 10^{53} erg, which is comparable to or a factor of two to three larger than the observed kinetic energy of the arm. This amount of energy is far less compared with the total energy, 10^{58-59} erg, required in the model of Sanders and Prendergast (1974). See Sofue (1976a) for detailed discussion of the energetics.

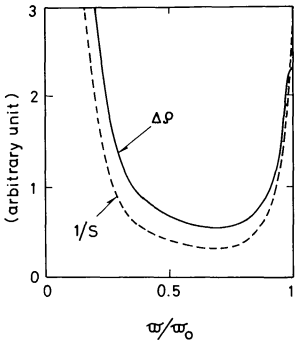

Fig. 5. Full line: excess of the density at the wave front over the unperturbed density plotted against the galactocentric distance. Broken line: inverse of surface area of the cross section of the wave duct given by Equation (11). Both are indicated in arbitrary units

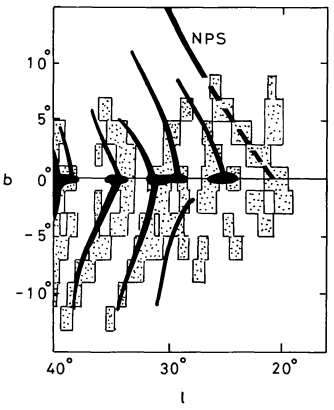

Fig. 6. Thick lines: ridges of galactic spurs at 408 MHz collected from the map of Haslam et al. (1974). Shaded areas: ridges of neutral hydrogen gas located along a locus of maximum radial velocity of the galactic rotation (Sofue et al., 1976). A smooth extension of the main ridge of the North-Polar-Spur indicated with a heavy, dashed line crosses the galactic plane at $l=21°$. Note that the NPS is associated with a H I ridge

V. Shell-like Front of the MHD Waves in the Galactic Corona

In this section, we subject the computed results in Case B to a comparison with observations of the galactic background emission. In particular, we are interested in a large arc structure in the radio continuum, namely, the North Polar Spur, and in an H I gas feature probably associated with the 3-kpc arm in the space above the galactic plane.

(i) The North Polar Spur

A number of authors have searched for counterparts of the North Polar Spur in the 21-cm H I line, in X-rays, in Hα emission and in starlights (Berkhuijsen et al., 1971; Davies et al., 1963; Sofue, 1973; Sofue et al., 1974; Bunner et al., 1972; de Korte et al., 1974; Kato, 1973; Heiles and Jenkins, 1976). In spite of the efforts made so far, however, only crude correlations have been found between them. Worse still, their true spatial relations are far from clear because of uncertainties in distances of various features in the line-of-sight. Furthermore, the interpretation of these correlations remains controversial (Sofue et al., 1974). It seems therefore still worthwhile to examine further possibility to interpret the NPS.

(ii) Radio Continuum and H I*-gas Features near the* 3-kpc *Arm*

Haslam et al. (1974) have given a high-resolution map of the radio continuum background at 408 MHz covering a wide area of the sky including the NPS. It reveals also many complicated structure near the galactic plane, especially a number of spurs emerging from the galactic plane. Figure 6 shows ridge lines of spurs collected from this map at $l=10-40°$, $b=-15-+15°$. A smooth extension of the main ridge of the NPS, which is indicated with a heavy dashed line, crosses the galactic plane at $l=21°$.

We now turn our attention to H I gas features around the galactic center region. Lower part of Figure 7 shows a schematic structure of the central region of the Galaxy reproduced from Sanders and Wrixon (1973). There are several ring structures of gas in this region. They have widely accepted to be the result of galactic center activities. The outermost ring located at $\varpi=3.5$ kpc is the wellknown 3-kpc arm.

We must note that the direction tangential to this ring from the sun is at $l=21°$, which exactly coincides with the crossing point of the smooth extension of NPS

with the galactic plane, $l=21°$. This apparent coincidence seems too close to be regarded as merely accidental, but rather suggests a physical connection of the 3-kpc arm to the NPS.

Figure 6 shows cross sections of spiral arms of HI gas cut along the locus of maximum radial velocity of galactic rotation using the data by Burton and Verschuur (1973). A detailed description and interpretation of many characteristic features appearing in this figure have been given in Sofue et al. (1976). We here notice the fact that the smooth extension of the NPS ridge is associated with an HI-gas ridge which extends to positive latitudes from an HI-gas condensation at $l=21°$, $b=0°$. The HI gas in this ridge has a radial velocity of 120 km s^{-1}, indicating that the gas is located at $\varpi=3.5$ kpc. This coincidence suggests a physical association of the 3-kpc arm with this HI structure.

(iii) Is the NPS *a* MHD *Shock Front from the Active Galactic Center?*

In Section II (ii), we have shown that the MHD wave front from the galactic center forms a large shell-structure in the galactic corona (Fig. 2). In Figure 7, we superpose the tangential view of the wave front as seen from the sun at $t=1.7$ and $1.8\,10^8$ years for $\alpha=0.5$ ($V_\infty=150$ km s^{-1}) on the 820 MHz radio continuum map reproduced from Berkhuijsen (1972). For $b<60°$, good fit of the computed MHD front to the NPS ridge is obtained at $t=1.8\ 10^8$ years, at which time the convergence ring appears at $\varpi=3.5$ kpc corresponding to the 3-kpc arm. Thus, insofar as the geometry of the wave front is concerned, the MHD front can reasonably reproduce the NPS ridge. The fit is best when the Alfvén velocity in the high corona is taken as $V_\infty=150$ km s^{-1} ($\alpha=0.5$). Figure

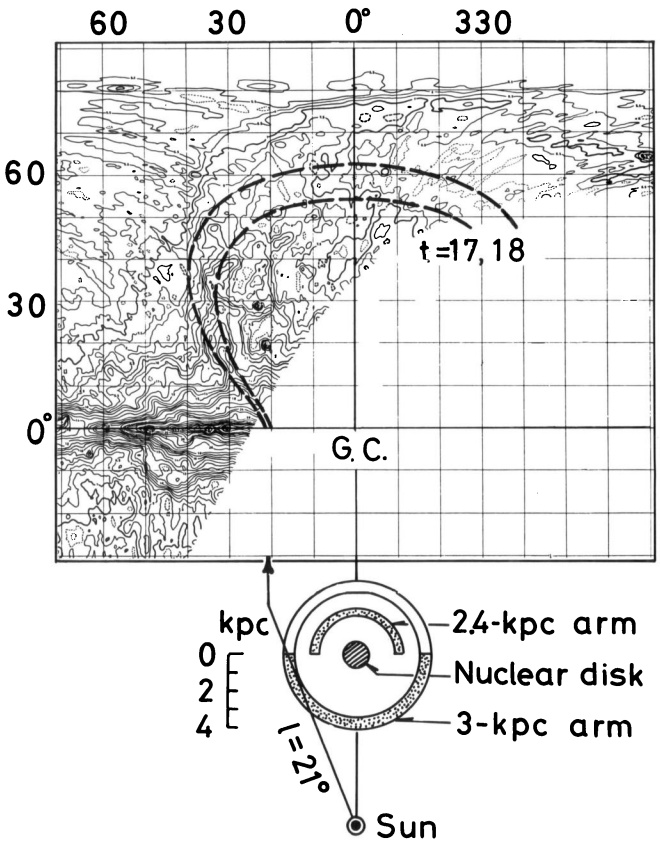

Fig. 7. Tangential projection of the MHD wave front at $t=17$–18.10^7 years in Case B ($\alpha=0.5$, $V_\infty=150$ km s^{-1}; dashed lines) on the (l, b)-plane superposed on the 820 MHz map of the background radio emission from Berkhuijsen (1972). For $b<60°$ the North-Polar-Spur is reasonably well fitted by the wave front. Also illustrated is a schematic ring structure of HI gas in the central region of the Galaxy as seen from the North Galactic Pole. Note that the tangential direction of the 3-kpc arm seen from the sun is at $l=21°$, which is close to the position where the smooth extension of the NPS crosses the galactic plane

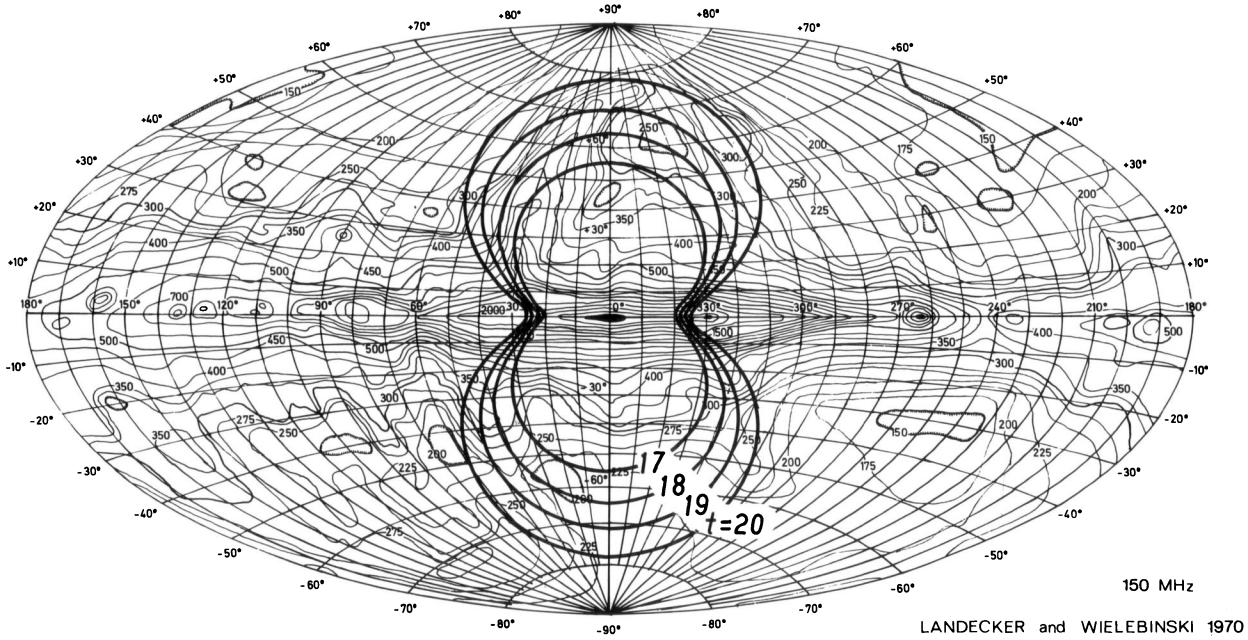

Fig. 8. The same as Figure 7, but for the front at $t=17-20.10^7$ years superposed on the 150 MHz map by Landecker and Wielebinski (1970)

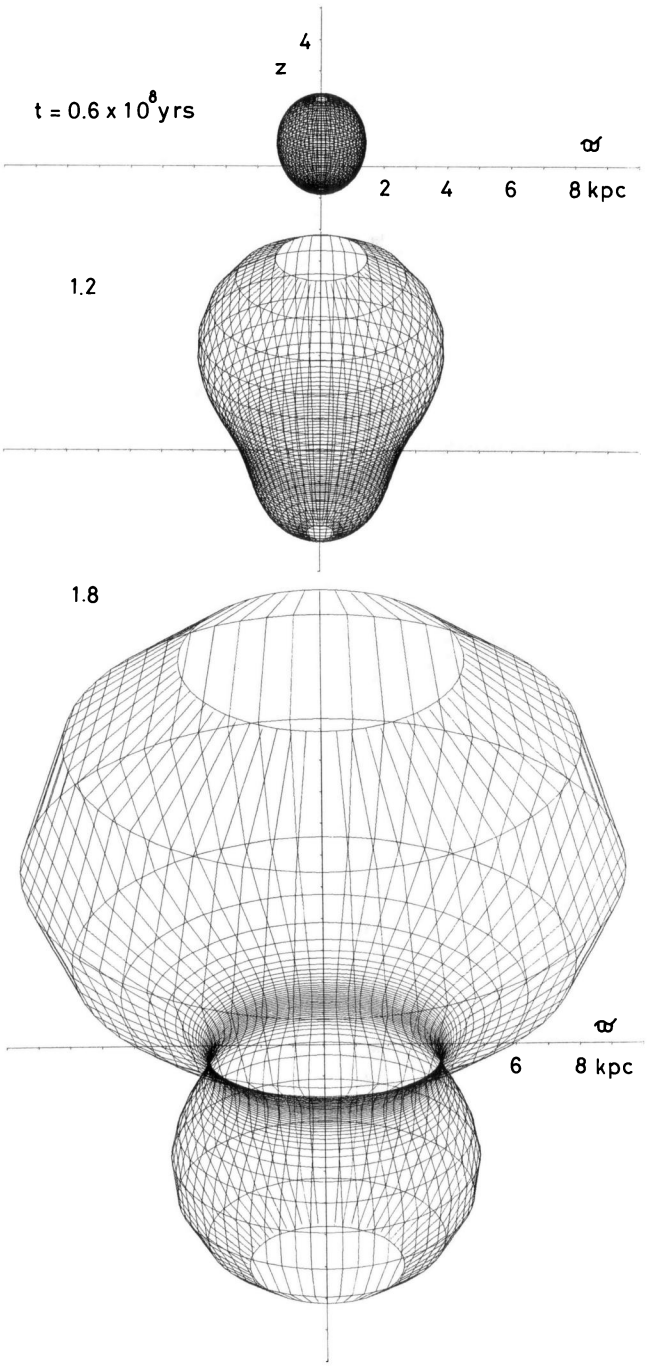

Fig. 9. The same as Figure 2a, but for an explosion at a height of $z=800$ pc above the galactic plane

8 compares our MHD front at $t=0.7-2.0\,10^8$ years with an overall distribution of the radio continuum emission of the Galaxy at 150 MHz (Landecker and Wielebinski, 1970). We find some further possible association of spurs with the front at $t\approx 1.8\,10^8$ years: a spur emerging from $(l,b)=(330°,-20°)$, a spur near $(40°,-40°)$, and a hump near $(320°, 25°)$, although the fit is still rough compared with the case of NPS. However, it would be possible to fit them better, if we take into account a more sophisticated distribution of the Alfvén velocity in the galactic corona.

The present computation of the MHD waves of small amplitude cannot give absolute values of the propagating energy and radio emissivity at the wave front in the galactic corona. Instead we make here an order-of-magnitude estimate for the energy involved in the NPS and the 3-kpc arm: Observed excess temperature at the NPS ridge at $(l,b)=(30°,30°)$ is $\Delta T=5°$ at 820 MHz. We can then estimate the emissivity in the NPS as $\varepsilon_\nu\approx 2k\nu^2\Delta T/Lc^2\approx 1\,10^{-40}$ erg cm^{-3} s^{-1} Hz^{-1} at $\nu=820$ MHz. Here we have taken a tangential line-of-sight depth of the front as $L\approx 3$ kpc, and its thickness as $\Delta L\approx 300$ pc. The total emissivity from the NPS in the radio wave range is then roughly evaluated as $E_r\approx L^2\Delta L\nu\varepsilon_\nu\approx 6\,10^{34}$ erg s^{-1}. The total energy emitted during the past $1.8-2\,10^8$ years since the nuclear explosion would be of the order of $E_r t\approx 1.6\,10^{50}$ erg. This is much smaller than the kinetic energy, 10^{52-53} erg, required for the point explosion at the nucleus (Paper I) to drive the expanding motion of the 3-kpc arm.

VI. Conclusions and Discussion

The MHD model for the 3-kpc arm proposed in Paper I has been improved using a more realistic model of the Alfvén velocity distribution in the galactic corona at high-z. Below we summarise the results:

i) Approximately 80% of the MHD waves isotropically radiated from the galactic center are reflected at the galactic corona. They converge into a focal ring in the galactic plane away from the center (Figs. 1–3). If the z-scale height of the Alfvén velocity distribution is taken as 1.7 kpc, the radius of the ring is 3.5 kpc. The galactic disk is considered as a wave duct to which the MHD wave propagation is confined: The wave duct guides the MHD waves into a thin, narrow focal ring.

ii) We followed a blast wave which propagates in the duct using a hydrodynamical code (Figs. 4 and 5). A strong shock from the galactic center is weakened to a small amplitude blast wave by the spherical damping, and is propagated almost without dissipation through the disk. At $\varpi=2-3$ kpc the disk is hardly disturbed by the passage of the wave.

When the wave approaches the focal ring, its amplitude increases rapidly due to a decrease of the cross section of the duct. As a consequence, a strong shock grows near the focus, which may be the cause of the 3-kpc arm.

iii) A small portion of the MHD waves from the galactic center escapes into the corona (Fig. 2). The front forms there a large shell structure. If the Alfvén velocity tends to a constant value of about 150 km s^{-1} at high-z ($z>2$ kpc), the tangential view of the shell at $t=1.8\,10^8$ years as seen from the sun reasonably fits the North-Polar-Spur ridge (Fig. 7). According to our MHD model,

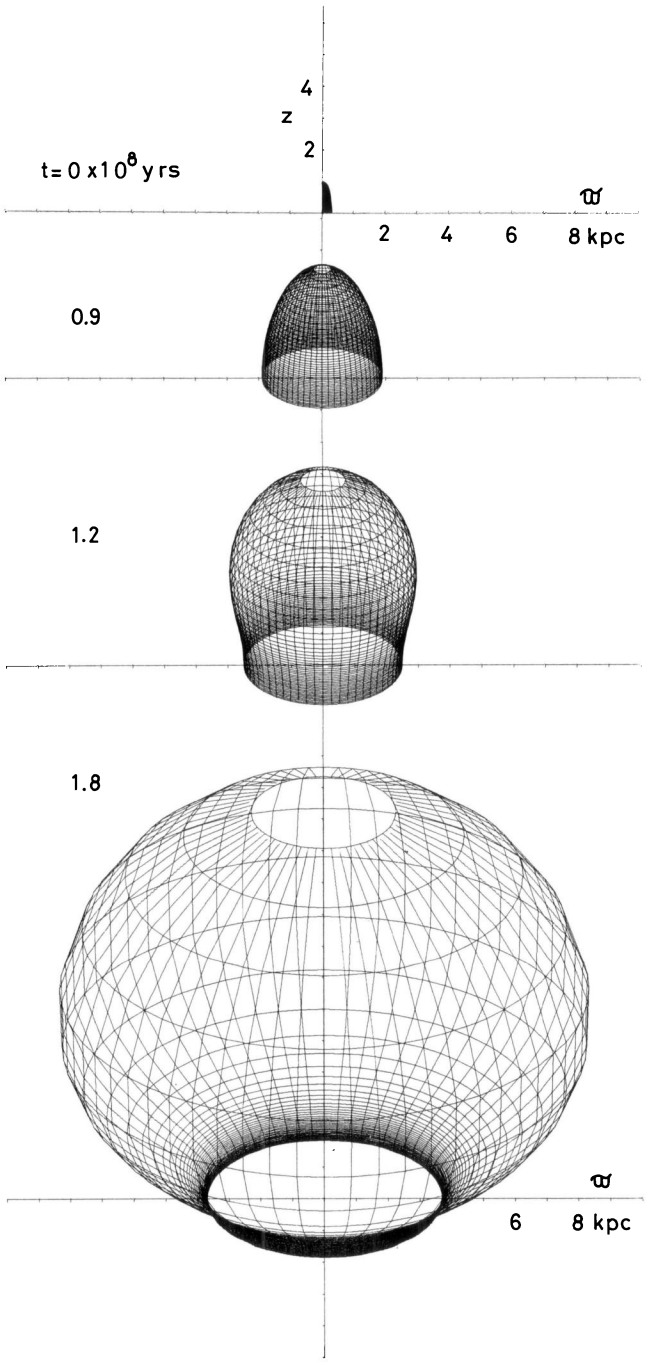

Fig. 10a. The same as Figure 2a, but for an anisotropic explosion from a surface elongated in the z-direction

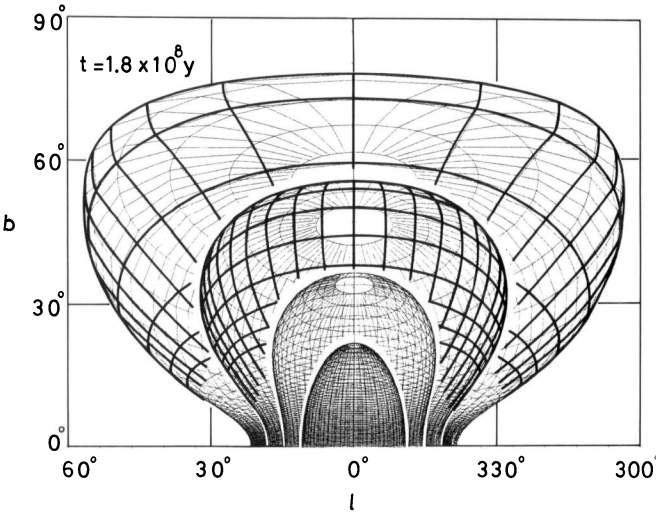

Fig. 10b. Projection on the sky of the MHD shell at $t=0.9$, 1.2, 1.5 and 1.8 10^8 years for the case in Figure 10a

the geometrical correlation of the NPS and the 3-kpc arm (Figs. 6 and 7) can be explained assuming both the galactic center activity and the existence of the galactic corona.

iv) However, except for the NPS at $b<60°$, the fit of the computed MHD shell to the spur is rather rough. Furthermore some other spurs possibly associated with the shell are far from symmetric around the galactic plane. Such an asymmetry, if the spurs are attributable to the galactic center activity, might suggest some anisotropic explosion and/or a deviation of the explosion point from the galactic center. In order to see how an asymmetry of the explosion affects the result, we have computed the following two cases:

(a) An isotropic explosion takes place above the galactic plane at the height of $z=z_0=800$ pc. Figure 9 shows the result. The front is spherical in the initial stage, and then elongated in the z-direction forming a pear-shaped front. Finally it forms two spherical shells of different radii above and below the galactic plane. Focusing into a ring also takes place for the near-plane waves, although the focal ring appears below the plane at $z=-z_0$.

(b) The explosion begins from a spindle-shaped surface elongated in the z-direction, so that it simulates an isotropic explosion perpendicular to the gaseous disk. The final front is similar to that in Case B of isotropic explosion, except that the front is more elongated in the z-direction (Fig. 10a). The focusing takes place also. The fitting to the NPS is, however, worse than in Case B of isotropic explosion, except for the improved fit at $b>50°$ (Fig. 10b).

Acknowledgements. The author expresses his thanks to Professor Dr. O. Hachenberg for giving the opportunity to stay at MPIfR and for reading of the manuscript. He thanks also Dr. E. M. Berkhuijsen for valuable discussions and reading of the manuscript. The present work was completed during a stay at MPI under the support by the Alexander von Humboldt-Stiftung. Numerical computations were made on a HITAC8500 at the Plasma Institute, Nagoya University, and on a CDC Cyber 172 at the MPI, Bonn.

References

Berkhuijsen, E.M.: 1972, *Astron. Astrophys. Suppl.* **5**, 263
Berkhuijsen, E.M., Haslam, C.G.T., Salter, C.J.: 1971, *Astron. Astrophys.* **14**, 252
Bunner, A.N., Coleman, P.L., Kraushaar, W.L., McCammon, D.: 1972, *Astrophys. J. Letters* **172**, L67
Burton, W.B., Verschuur, G.L.: 1973, *Astron. Astrophys. Suppl.* **12**, 145

Davies, R., Hanbury Brown, R., Meaburn, J.: 1963, *Observatory* **83**, 179
de Korte, P. A. J., Bleeker, J. A. M., Deerenberg, A. J. M., Tanaka, Y., Yamashita, K.: 1974, *Astrophys. J.* **190**, L5
Haslam, C. G. T., Wilson, W. E., Graham, D. A., Hunt, G. C.: 1974, *Astrophys. Suppl.* **13**, 359
Heiles, C., Jenkins, F. B.: 1976, *Astron. Astrophys.* **46**, 333
Kato, T.: 1973, *Astrophys. Space Sci.* **12**, 789
Landecker, T. L., Wielebinski, R.: 1970, *Australian J. Phys.* **16**, 1
Lynden-Bell, D., Rees, M.: 1971, *Monthly Notices Roy. Astron. Soc.* **152**, 461
Moreton, G. E.: 1960, *Astron. J.* **65**, 491
Parker, E. N.: 1969, Space Sci. Rev. **9**, 651
Richtmeyer, R. D.: 1957, Difference Methods of Initial Value Problem, New York; Interscience Publishers
Rougoor, G. W.: 1964, *Bull. Astron. Inst. Neth.* **17**, 381
Saito, M.: 1976, Preprints
Sanders, R. H., Prendergast, K. H.: 1974, *Astrophys. J.* **188**, 489
Sanders, R. H., Wrixon, G. T.: 1973, *Astron. Astrophys.* **26**, 365
Simonson, S. C., Mader, C. L.: 1973, *Astron. Astrophys.* **27**, 337
Sofue, Y.: 1973, *Publ. Astron. Soc. Japan* **25**, 207
Sofue, Y.: 1976a, *Publ. Astron. Soc. Japan* **28**, 19
Sofue, Y.: 1976b, *Astron. Astrophys.* **48**, 1
Sofue, Y., Fujimoto, M., Tosa, M.: 1976, *Publ. Astron. Soc. Japan* **28**, 317
Sofue, Y., Hamajima, K., Fujimoto, M.: 1974, *Publ. Astron. Soc. Japan* **26**, 399
Uchida, Y.: 1968, *Solar Phys.* **4**, 30
Uchida, Y.: 1970, *Publ. Astron. Soc. Japan* **22**, 341
Uchida, Y.: 1974, *Solar Phys.* **39**, 431
Uchida, Y., Altschuler, M. D., Newkirk, H., Jr.: 1973, *Solar Phys.* **28**, 495
van der Kruit, P. C.: 1971, *Astron. Astrophys.* **13**, 405
Woltjer, L.: 1965, in Galactic Structure, ed. A. Blaauw and M. Schmidt, The University Chicago Press, Chicago, p. 531